Spring 2019

CD47 Blockade Enhances Macrophage Efferocytosis Via a Process Requiring Low-Density Lipoprotein Receptor-Related Protein 1

Richard Anthony Maldonado
Concordia University - Portland, ramaldon@icloud.com

CD47 Blockade Enhances Macrophage Efferocytosis Via a Process Requiring Low-Density Lipoprotein Receptor-Related Protein 1

A senior thesis submitted to
The Department of Math-Science
College of Arts & Sciences

In partial fulfillment of the requirements
for a Bachelor of Arts degree in Biology

by

Richard Anthony Maldonado

Faculty Supervisor _____		_____
	Dr. Mihail Iordanov	**Date**
Department Chair _____		_____
	Dr. Mihail Iordanov	**Date**
Dean, College of Arts and Science _____		_____
	Dr. Michael Thomas	**Date**
Provost _____		_____
	Dr. Michelle Cowing	**Date**

Concordia University
Portland, Oregon
April, 2019

Table of Contents

Abstract

Vulnerable atherosclerotic plaques are characterized by large necrotic cores caused by impaired clearance of apoptotic cells (efferocytosis) in the artery wall. Targeted antibody blockade of CD47 (αCD47), an anti-efferocytosis protein, enhances efferocytosis and reduces plaque area in mouse models of atherosclerosis. LDL receptor-related protein-1 (LRP1) is a pro-efferocytosis receptor whose deletion from macrophages accelerates atherogenesis. We recently found that αCD47 requires macrophage LRP1 to limit atherosclerosis. Thus, we hypothesize that the enhanced efferocytosis caused by αCD47 also requires macrophage LRP1. We conducted *in vitro* studies using wildtype (WT) and $LRP1^{-/-}$ macrophages as efferocytes and either Jurkat lymphocyte cells or WT and $LRP1^{-/-}$ murine macrophages as apoptotic cell substrates (ACs). To stimulate efferocytosis, violet fluorescent-labeled apoptotic cells were co-incubated with green fluorescent-labeled efferocytes in the presence of αCD47 (10μg/mL) or IgG control. Phagocytic index (PI) is determined using confocal microscopy and flow cytometry as the percent of efferocytes with internalized ACs. In experiments using Jurkat cells as ACs, αCD47 increased PI 2.4-fold and 2.0-fold in WT and $LRP1^{-/-}$ efferocytes, respectively, compared to IgG control. No differences in PI were observed between WT and $LRP1^{-/-}$ efferocytes treated with αCD47 or IgG control. In experiments using WT and $LRP1^{-/-}$ macrophages as ACs, we observed no differences in PI between WT and $LRP1^{-/-}$ efferocytes. Interestingly, the use of $LRP1^{-/-}$ macrophages as ACs reduced the PI of WT efferocytes by 44.7% relative to WT macrophage ACs and independently of αCD47. These data suggest that the loss of LRP1 on ACs, not the efferocyte, impairs efferocytosis independently of αCD47 by rendering the dying cells a poor substrate for clearance.

CD47 Blockade Enhances Macrophage Efferocytosis Via a Process Requiring Low-Density Lipoprotein Receptor-Related Protein 1

Introduction

Atherosclerosis is a progressive inflammatory disease of the arteries, the underlying cause of myocardial infarction (MI) and cerebrovascular accident (CVA), the leading causes of death worldwide (WHO, 2018). Atherosclerotic plaques develop progressively throughout an individual's lifetime and can become vulnerable to rupture. A key feature of vulnerable plaques is the formation of a necrotic core (NC). The NC contains cellular debris and lipids originating from apoptotic cells which have undergone secondary necrosis as a result of their impaired removal through efferocytosis (Linton et al., 2015; Tabas, 2016). By studying the pathogenesis and resolution of the necrotic core via efferocytosis, novel treatments can be created to lower the mortality rate of atherosclerotic sequelae MI and CVA.

In healthy individuals, the arteries are primarily composed of the endothelium (intima), sub-endothelial region, a layer of smooth muscle cells (media), and adventitia (Fig. 1). The endothelium is the inner-most layer and is composed of a single layer of simple squamous endothelial cells connected by tight junctions to prevent leakage of circulating blood from the lumen where blood flows (Saladin, 2012).

There are two common types of blood flow, laminar and turbulent flow. Laminar flow occurs in regions where blood flows in a straight line, free of branching. In areas of laminar flow, endothelial cells exhibit coaxial alignment and synthesize compounds which promote endothelial health and atherosclerosis resistance. In contrast, areas of curvature, branching, and bifurcation have turbulent flow, and endothelial cells present

polymorphic structure and disordered alignment leading to a susceptibility to atherosclerosis (Linton et al., 2015). These athero-susceptible regions also show an increased inflammatory response (Linton et al., 2015).

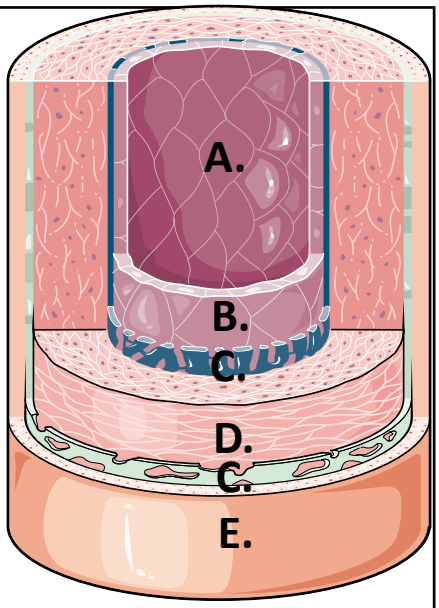

Figure 1. General Anatomy of an Artery. **A.** The lumen is the opening of the artery where blood flows. **B.** The intima is a single layer of endothelial cells. Immediately underneath it is the sub-endothelial space where atherosclerosis develops. **C.** The elastic lamina can be present in both positions, as shown, depending on the size of the artery. They give the arteries elasticity to compensate for the dynamic nature of blood flow in the arteries. **D.** The media is a multilayer region composed of smooth muscle cells. It's contribution to atherosclerosis is significant, though it will not be covered in this text. **E.** The externa (adventitia) is a layer primarily composed of collagen on the outermost portion of the blood vessel.

Atherosclerosis is initiated (Fig. 2) by the deposition and retention of apolipoprotein B (ApoB) containing lipoproteins (LDL), from circulation, into the subendothelial region of athero-susceptible areas of the arteries. The ApoB component of LDL interacts with proteoglycans in the subendothelial matrix and becomes trapped. Trapped LDL can undergo modification by interactions with reactive oxygen species (ROS) leading to the formation of oxidized LDL (ox-LDL). The LDL and ox-LDL incite an inflammatory response by the overlying endothelium.

One common inflammatory response is the upregulation of nuclear transcription factors in the nucleus of the endothelial cells which cause the presentation of monocyte adherent proteins on the luminal side of the endothelium. Monocytes present in the blood roll along the endothelium, attach to the adherent proteins, and migrate into the

subendothelial space (Kasikara, Doran, Cai, & Tabas, 2018; Linton et al., 2015; Moore & Tabas, 2011).

Monocytes differentiate into macrophages and begin the process of LDL and Ox-LDL uptake, and conversion to HDL (efflux) by way of reverse cholesterol transport. Initially, the clearance of LDL is likely beneficial (Moore, Sheedy, & Fisher, 2013) however, there is a net influx of LDL/Ox-LDL which overwhelms the efflux mechanism leading to the formation of lipid-laden foam cell macrophages.

Foam cells are characterized by a decreased ability to migrate out of the sub-endothelial space, leading to an increased inflammatory response and advanced complex plaques (Moore et al., 2013). Foam cells, with their decreased ability to emigrate out of

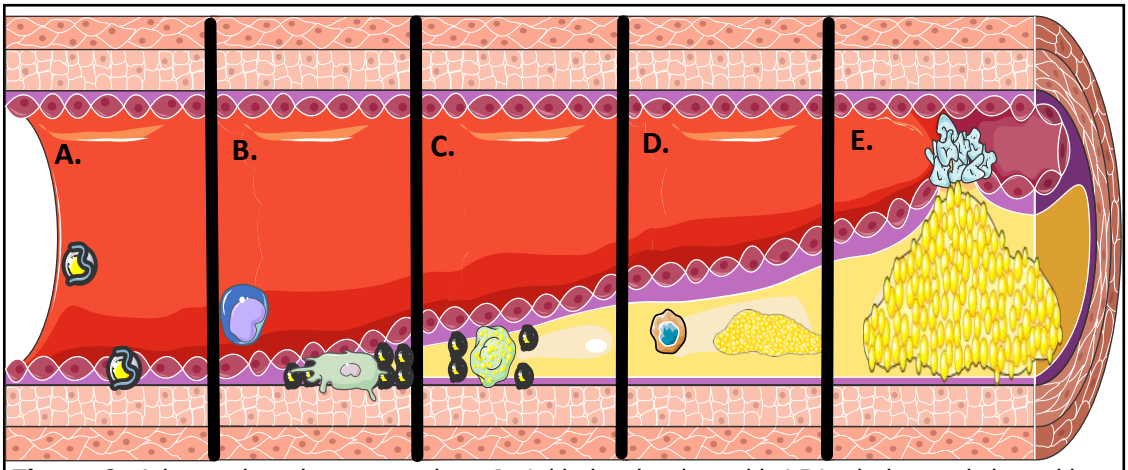

Figure 2. Atherosclerosis progression. **A.** Initiation begins with LDL-cholesterol depositing into the subendothelial region between the endothelium (intima) and smooth muscle cells (media) of the artery wall. **B.** Activation of the endothelium leads to monocyte recruitment into the subendothelial space where they differentiate into macrophages and begin phagocytosing LDL. **C.** Macrophages uptake cholesterol faster than they can process it through reverse cholesterol transport and become macrophage foam cells. **D.** Foam cells undergo programmed cell death (apoptosis) and are not efficiently cleared through efferocytosis. The apoptotic foam cells undergo secondary necrosis and contribute their contents to the plaque forming a necrotic core. **E.** There is little negative feedback and the cycle repeats resulting in the growth of the necrotic core. Eventually, the plaque ruptures leading to the formation of a thrombus in the lumen. The thrombus cuts off blood flow downstream causing infarction which leads to tissue death downstream of the thrombus.

the cell wall, undergo programmed cell death (apoptosis) likely as a result of endoplasmic reticulum stress (Seimon & Tabas, 2009).

In atherosclerosis, apoptosis is dysregulated, and cell death occurs at an accelerated rate due to the highly toxic environment in advanced plaques (Linton et al., 2015). Apoptosis is normally resolved through programmed cell removal, known as efferocytosis (Elliott, Koster, & Murphy, 2017). In the early stages of atherosclerosis, the rate of clearance appears to be conserved due to low the low levels of apoptotic cells present in the plaque (Seimon & Tabas, 2009; Tabas, 2010). However, in advanced plaques, the necrotic core (NC) shows a high level of macrophage debris and lipid content, leading to the conclusion that post-apoptotic (necrotic) foam cells are a driving force in the development of the NC and instability of advanced plaques. Post-apoptotic necrosis involves leaky membranes and organelle swelling leading to complete cellular death (Seimon & Tabas, 2009). Thus, necrotic foam cells contribute their lipid contents and cellular debris to the NC.

Under normal conditions, the body can remove upwards of one-million apoptotic cells per second (Kojima, Weissman, & Leeper, 2017). Efferocytosis is a highly conserved and regulated process to prevent off-target removal of healthy tissue (Kojima et al., 2017). However, in atherosclerosis, this process is dysregulated leading to an accumulation of post-apoptotic cellular debris as mentioned above (Kojima et al., 2017).

Efferocytosis involves the engulfment (phagocytosis) of whole apoptotic cells by either professional (macrophages) or non-professional (dendritic cells, smooth muscle cells) efferocytes. Several molecules have been implicated in the balance of efferocytosis signaling (Fig. 3). Efferocytosis signaling can be categorized into the, “don’t eat me,” “find me,” and “eat me” stages.

Healthy cells express anti-efferocytosis "don't eat me" signals such as CD47, an integrin-associated cell surface protein which prevents immune cells from marking healthy cells for removal. CD47 interacts with the transmembrane protein SIRPα found on the surface of the engulfing cell, inhibiting efferocytosis (Gardai et al., 2005). CD47 is overexpressed in malignant tumors, and anti-CD47 (αCD47) antibodies have been shown to have a positive effect on malignant tumor regression (Majeti et al., 2009). As a result, CD47 became a subject of study in atherosclerosis where it has been shown to be

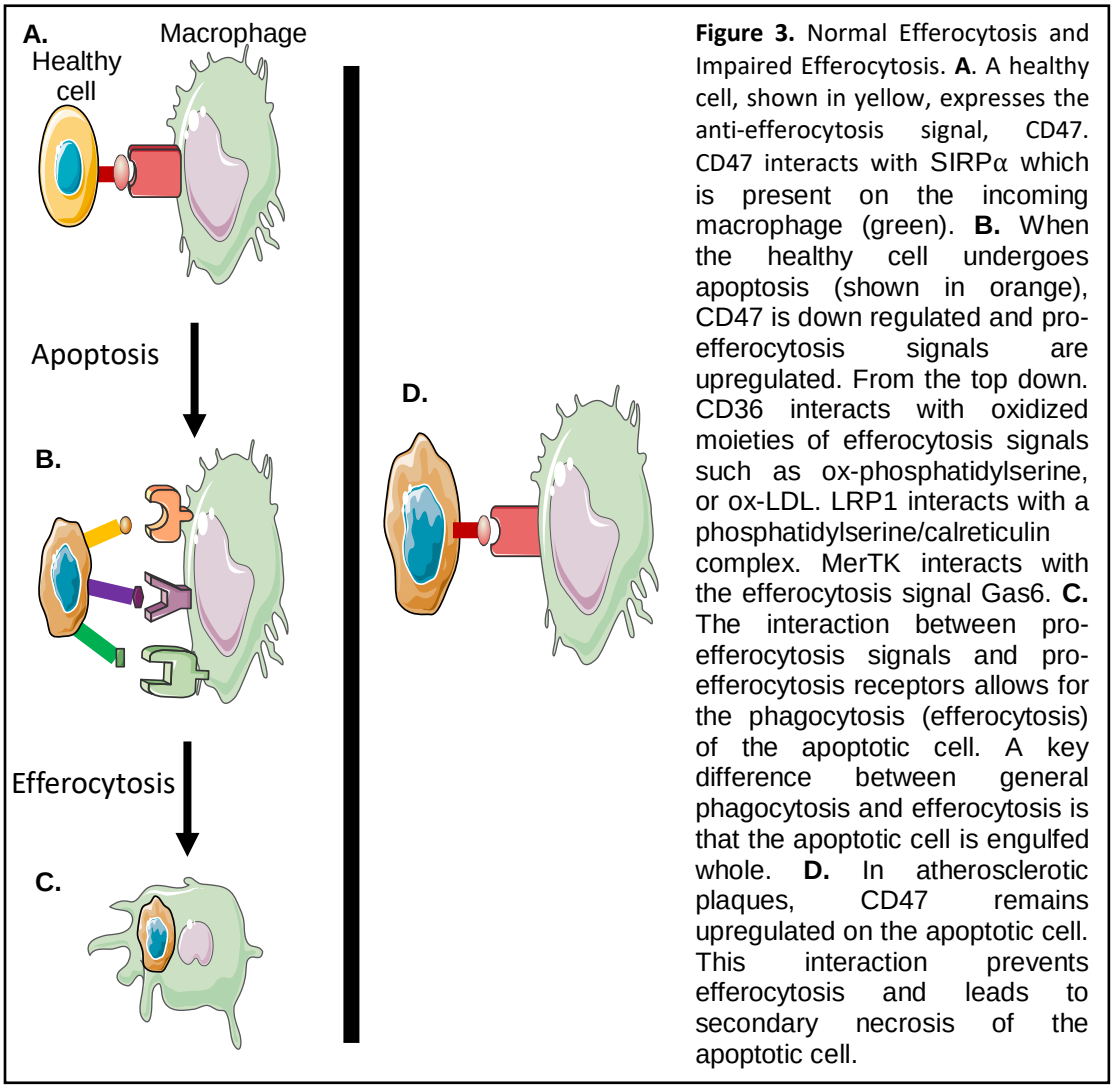

Figure 3. Normal Efferocytosis and Impaired Efferocytosis. **A**. A healthy cell, shown in yellow, expresses the anti-efferocytosis signal, CD47. CD47 interacts with SIRPα which is present on the incoming macrophage (green). **B.** When the healthy cell undergoes apoptosis (shown in orange), CD47 is down regulated and pro-efferocytosis signals are upregulated. From the top down. CD36 interacts with oxidized moieties of efferocytosis signals such as ox-phosphatidylserine, or ox-LDL. LRP1 interacts with a phosphatidylserine/calreticulin complex. MerTK interacts with the efferocytosis signal Gas6. **C.** The interaction between pro-efferocytosis signals and pro-efferocytosis receptors allows for the phagocytosis (efferocytosis) of the apoptotic cell. A key difference between general phagocytosis and efferocytosis is that the apoptotic cell is engulfed whole. **D.** In atherosclerotic plaques, CD47 remains upregulated on the apoptotic cell. This interaction prevents efferocytosis and leads to secondary necrosis of the apoptotic cell.

upregulated in atherosclerotic plaques. Furthermore, a CD47 antibody blockade has been shown to prevent atherosclerosis via increased efferocytosis (Kojima et al., 2016).

Efferocytosis initiation occurs when an apoptotic cell expresses chemoattractant "find me" ligands. In addition to recruiting both professional and non-professional efferocytes, these ligands are also responsible for decreasing expression of a cell's "don't eat me" signals and rapidly upregulating the expression of "eat me" signals (Tabas, 2010).

Pro-efferocytosis "eat me" signals are expressed on the surface of apoptotic cells. Several pro-efferocytosis "eat me" signals and bridging molecules have been identified. In one example, calreticulin, a chaperone protein, is upregulated on the surface of apoptotic cells. Calreticulin forms a complex with phosphatidylserine on the surface of the apoptotic cell. This complex interacts with the pro-efferocytosis receptor low-density lipoprotein receptor-related protein 1 (LRP1), allowing phagocytosis of the apoptotic cell (Kojima et al., 2017).

Pro-efferocytosis receptors are found on the surface of both professional and non-professional efferocytes. Several cell-surface "eat me" receptor proteins and have been identified such as CD36, MerTK, and the subject of this study, LRP1 (Fadok, Warner, Bratton, & Henson, 1998; Thorp, Cui, Schrijvers, Kuriakose, & Tabas, 2008; Yancey et al., 2011). When activated, pro-efferocytosis receptors allow for engulfment of the apoptotic cell by the efferocyte. Recently, it has been shown that the loss of macrophage LRP1 accelerates atherosclerosis progression, leading to larger plaques, increased necrotic core size, and decreased efferocytosis (Overton, Yancey, Major, Linton, & Fazio, 2007; Yancey et al., 2010; Yancey et al., 2011).

Based on these previous studies, Fazio lab conducted experiments to ascertain what effect the loss LRP1, present on the efferocyte, had on efferocytosis in the presence of a CD47 antibody blockade (αCD47). They conducted *in vivo* experiments on athero-susceptible ($ApoE^{-/-}$), and $ApoE^{-/-}$/macrophage specific LRP1 ($M\Phi LRP1^{-/-}$) double knockout mice fed a high-fat diet for 12 weeks. Both groups of mice were treated with a

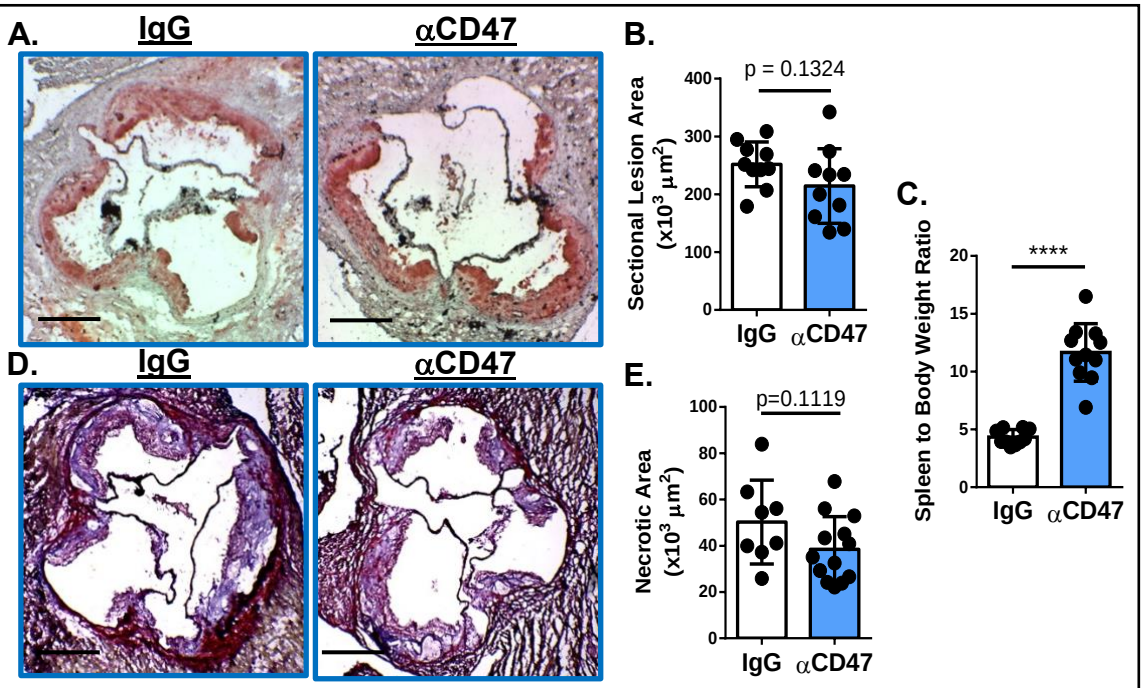

Fig 4. Macrophage $LRP1^{-/-}$/$ApoE^{-/-}$ double knockout mice were fed a high-fat (Western) diet while receiving anti-CD47 blocking antibody (200μg/injection) or IgG control every other day for 12 weeks. (A) and (B) aortic sinus sections were stained with oil red-O lesion area quantified. (C) Spleen weight to body weight ratio. (D) and (E) necrotic core area was determined in aortic sinus sections using Mason's Trichrome stain and acellular area quantified. *P<0.05; ****P<0.0001. Figure courtesy of Paul Mueller, Ph.D.

CD47 blocking antibody or IgG control on alternating days for twelve weeks. Mice were euthanized, and cross sections of the aortic sinus were removed. The lesion and necrotic core areas of the aortic sinus were then measured and quantified. The results show that the double knockout ($ApoE^{-/-}$/ $M\Phi LRP1^{-/-}$) mice had larger lesions and larger necrotic

cores when compared to the ApoE$^{-/-}$ mice (Fig. 4 & 5). Spleen to body weight ratio was measured as a way to verify the effects of αCD47. Young erythrocytes express high levels of CD47, and a CD47 blockade prevents efferocytosis of apoptotic erythrocytes.

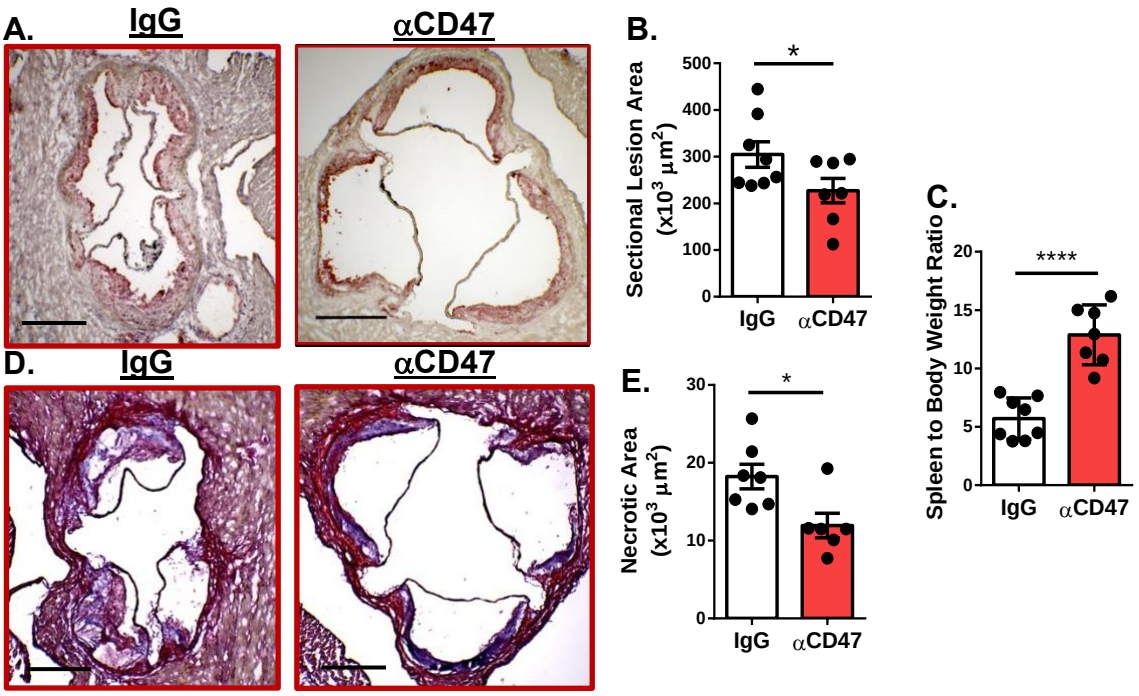

Fig 5. ApoE$^{-/-}$ mice were fed a high fat while receiving anti-CD47 blocking antibody (200μg/injection) or IgG control every other day for 12 weeks. (A) and (B) aortic sinus sections were stained with oil red-O lesion area quantified. (C) Spleen weight to body weight ratio. (D) and (E) necrotic core area was determined in aortic sinus sections using Mason's Trichrome stain and acellular area quantified. *P<0.05; ****P<0.0001. Figure courtesy of Paul Mueller, Ph.D.

Apoptotic erythrocytes accumulate in the spleen. Therefore, mice receiving an αCD47 treatment have a larger spleen ratio compared to the no-treatment group.

Because of these findings, we hypothesized that the enhanced efferocytosis imparted by an αCD47 blockade, requires macrophage LRP1. To test this hypothesis, we conducted *in vitro* studies using J774, and WT or LRP1$^{-/-}$ macrophages as efferocytes. Jurkat lymphocytes were used as apoptotic cell substrates (ACs). Additional experiments involved testing LRP1$^{-/-}$ macrophages as substrates for efferocytosis, this involved *in vitro* studies using either WT or LRP1$^{-/-}$ macrophages as either efferocyte or ACs. Further

experiments were also conducted to measure protein expression of select pro-efferocytosis receptors in WT and LRP1$^{-/-}$ macrophages.

Methods

Cells

For *in vitro* assay development, we used murine derived J774 macrophages as efferocytes and human-derived Jurkat T-lymphocytes as apoptotic substrate. Both cell types were incubated in Corning T-75cm^2 flasks at 37°C. J774's were cultured in 10% FBS, 1% penicillin/streptomycin, Gibco® 1X Dulbecco's Modified Eagle Medium (DMEM). Jurkat cells were incubated in 10% FBS, 1% penicillin/streptomycin, Gibco® 1640 Rosewell Park Memorial Institute (RPMI) + Glutamax™ media. Cells were passaged at approximately 80-90% confluency.

For efferocytosis and substrate experiments peritoneal primary macrophages were obtained from either WT or MΦLRP1$^{-/-}$ mice who had received thioglycolate injections to the abdomen five days prior to cell extraction. Cell extraction was performed, and cells were seeded directly into 12 or 24-well plates (1x10^6 cells/well) in 10% FBS, 1% pen/strep, DMEM, and incubated at 37°C. All experiments involving mice were carried out according to and with approval from Oregon Health & Science University's Institutional Animal Care and Use Committee (IACUC).

Immunohistochemistry

Immunohistochemical fluorescent probes were used in order to perform confocal and fluorescence-activated cell sorting for efferocytosis quantification. Macrophages were labeled with Invitrogen™ Vybrant® carboxyfluorescein diacetate, succinimidyl ester (CFDA SE) green cell tracker. Macrophages assigned for confocal microscopy were

incubated overnight in 12-well plates containing poly-L-lysine 12mm round coverslips. The CFDA SE was reconstituted in 90μL DMSO for a working solution of 10mM. Cells were washed two times with pre-warmed 1X-PBS, then incubated in 1X PBS containing 5 μM CFDA SE for 15 minutes at 37°C. Cells were then washed two times with pre-warmed 1X-PBS. DMEM containing 10% FBS/1% penicillin/streptomycin was replaced in the wells and cells were incubated at 37°C for 30 minutes.

Apoptotic cells were labeled with Invitrogen™ CellTracker™ Violet BMQC (2,3,6,7-tetrahydro-9- bromomethyl-1H,5H- quinolizino(9,1-gh)coumarin), for fluorescence-activated cell sorting, or Invitrogen™ CellTracker™ Red CMTPX ($C_{42}H_{40}ClN_3O_4$) cell dye, for confocal microscopy. Violet BMQC was reconstituted in 29.9μL DMSO for a concentration of 10mM. Red CMTPX was reconstituted in 7.28μL of DMSO for a concentration 10mM. Jurkat cells were centrifuged at 1,100 rpm for 10 minutes. Media was removed and replaced with serum-free DMEM containing 5μM Violet BMQC, or Red CMTPX, and cells were incubated at 37°C for 30 minutes. After 30 minutes, cells were centrifuged and washed in pre-warmed 1X-PBS with a cell count performed at this step. Cells were centrifuged and resuspended in phenol-free/serum-free DMEM. Jurkat cells were then seeded into 6-well plates at $3x10^6$ cell/well.

Confocal Microscopy

Confocal microscopy was conducted using a Nikon A1R microscope. Efferocytosis was quantified by manually counting cells in the open source software, ImageJ. To determine phagocytic index (PI) the image was divided into grids and portions of the grid were randomly selected. Then green macrophages and green macrophages containing a red apoptotic cell were counted in the selected portions. If one

macrophage was in contact with or contained multiple apoptotic cells; or if multiple macrophages were in contact with one apoptotic cell, then each was counted as a separate efferocytosis event (Fig. 7 in results section).

Fluorescence Activated Cell Sorting – Flow Cytometry

Flow cytometry was conducted on the BD Biosciences LSR II flow cytometer. Green fluorescence was measured on the 488nm wavelength, and violet fluorescence was measured on the 405nm wavelength. Instrument software measured the forward scatter (FSC-A) distinguishing the size of the cells, and side scatter (SSC-A) which measures the granularity or complexity of the cells. Because macrophages are considerably larger than the apoptotic lymphocytes, this allowed us to easily distinguish between cell populations based on size (Fig. 6).

Cell populations were then "gated" according to their fluorescent intensity by utilizing green only CFDA-SE (488nm), violet only BMQC (405nm), and unlabeled cell populations. This allowed us to divide the scatter plot in the software into four quadrants, with green only cells in quadrant three, violet only cells in quadrant one, and unlabeled population in quadrant four.

To determine phagocytic index (PI), that is, the percent of total macrophages containing an apoptotic body, quadrant one (violet only) and quadrant four (unlabeled) were excluded from the measurements. Thus, the only cells counted were in the green population. Green labeled cells containing a violet signal (double positive) counted as efferocytosis and were present in quadrant two.

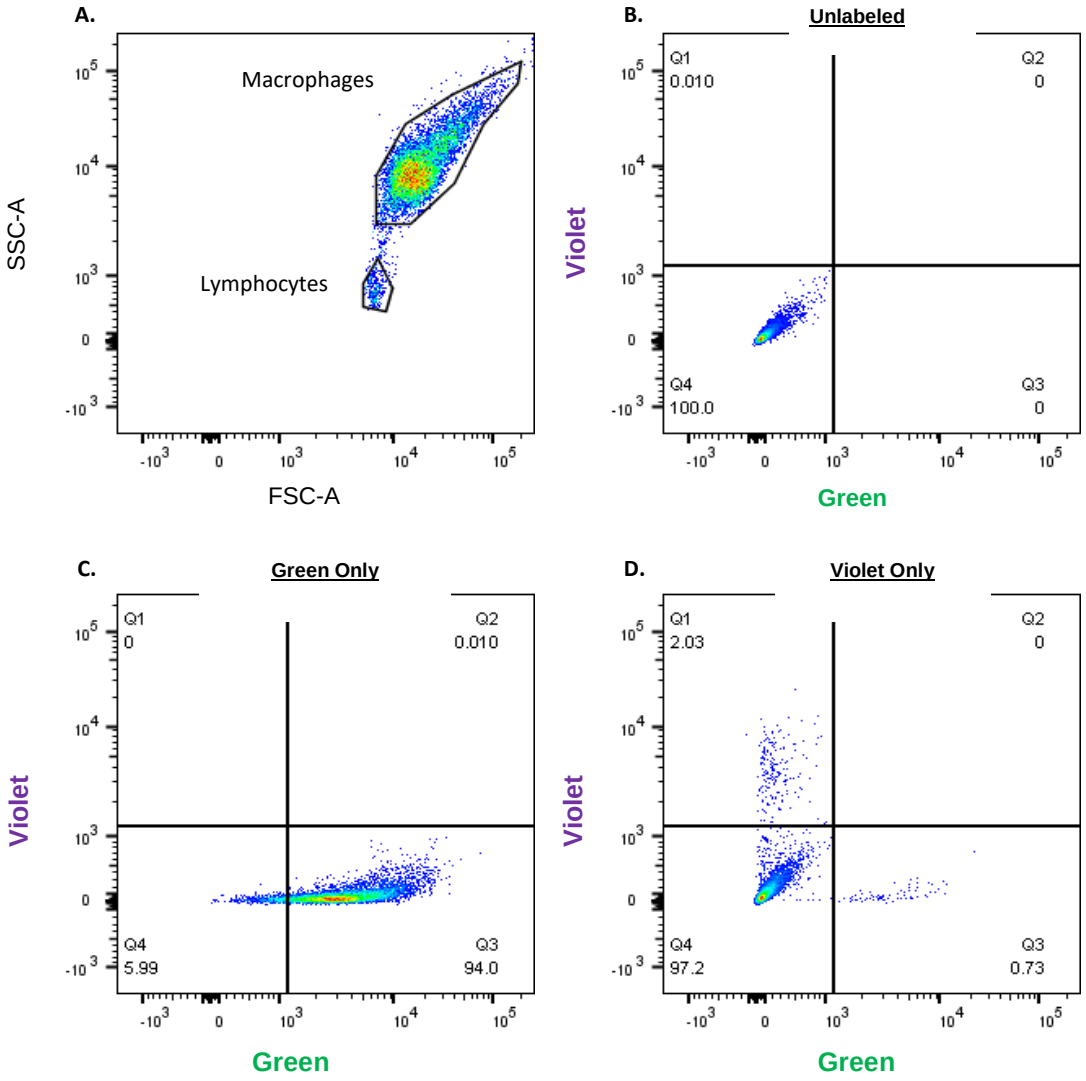

Figure 6. **A.** Side Scatter (SSC-A) shown on the y-axis measures the complexity of a cell based on its granularity and shape. Forward Scatter (FSC-A) shown on the x-axis and measures the size of the cell. **B.** Unlabeled cell populations present in quadrant 4 (Q4) and gated accordingly to exclude this population from the cell count. **C.** Green-only cells, measured in the 488nm wavelength, present in quadrant 3. **D.** Violet only cells, measured in the 405nm wavelength appear in quadrant 1. Phagocytic index was measured as the percent of total macrophages (green) containing an apoptotic body and appeared in quadrant two as a double positive signal (green and violet).

Western Blot

MerTK (110 kDa) expression was measured in WT and LRP1$^{-/-}$ macrophages to determine if the loss of LRP1 upregulated other pro-efferocytosis receptors. Protein was

extracted from cells, and Lowry assay was conducted to determine protein concentration. Protein mixture was prepared at 30μg in Thermo-Fisher Scientific invitrogen NuPage™ LDS Sample Buffer, Thermo-Fisher Scientific invitrogen NuPage™ Sample Reducing Agent, and deionized water. Protein samples (30μg) were loaded into Thermo-Fisher Scientific Invitrogen NuPage™ 4-12% Bis-Tris Gel (1.0 mm x 10 well). Electrophoresis was started at 100-volts for approximately 10 minutes, then at 120-volts for one and a half hours. The gel was transferred on ice on to GE Healthcare Life Sciences Amersham Protran Premium 0.45μm nitrocellulose blotting membrane for two and a half hours at 28-volts. The blotting membrane was then placed in 5ml LI-COR Odyssey® blocking buffer (TBS) for one hour.

After blocking, the blocking buffer was removed, and R&D systems goat anti-mouse MerTK primary antibody (1:1000), and abcam rabbit anti-mouse vinculin (124 kDa) primary antibody (1:2500), in 5mL of Odyssey® blocking buffer were added to the membrane. The membrane was then placed on a rocker overnight at 4°C.

The next day, the primary antibody solution was removed, and the membrane was washed three times with Tris-buffered saline containing polysorbate 20 (TBST) for 10 minutes each time. After the washes, LI-COR secondary antibodies were added in 5ml Odyssey® blocking buffer. We used donkey anti-goat 800CW for MerTK to be read on the green channel (800nm). For vinculin, we used goat anti-rabbit 680RD to be read on the red channel (700nm). Fluorescence intensity was measured using the LI-COR Odyssey® CLx blot imager, and LI-COR ImageStudio™ software.

Experiments

Experiments took place over ten weeks during the summer of 2016 at the Knight Cardiovascular Institute – Center for Preventive Cardiology under the supervision of Sergio Fazio MD/Ph.D. (Director of the Center for Preventive Cardiology), and Paul Mueller Ph.D.

Prior to the induction of apoptosis, well conditions were assigned, and Jurkat cells were incubated with either CD47 antibody (αCD47) or IgG at a concentration of 10μg/mL, during induction of apoptosis. All experiments contained a no-treatment (NT) control. For anti-CD47/LRP1 efferocytosis experiments, apoptosis was induced in Jurkat cells in 6-well plates exposed to long wavelength ultraviolet light for 30 minutes. Plates were placed directly underneath light source at a distance of 10 cm. Apoptosis induction for LRP1 substrate experiments utilized staurosporine (1μM) protein kinase inhibitor in serum-free DMEM.

For αCD47/LRP1 versus WT experiments, efferocytosis was stimulated by co-incubating apoptotic violet labeled Jurkat cells (either NT, αCD47, or IgG) with J774, WT, or $LRP1^{-/-}$ green labeled macrophages. Macrophages were washed two times with pre-warmed 1X PBS, and $1x10^6$ Jurkat cells were placed directly into the wells, in serum-free DMEM, with the macrophages according to assigned conditions. Cells were co-incubated for 2 hours. After two hours wells were washed two times with pre-warmed PBS and fixed with 4% paraformaldehyde (PFA) for 15 minutes.

After fixing, wells assigned for FACS were placed in polystyrene round-bottom tubes and taken for flow cytometry either the same or next day. For wells containing

coverslips, for confocal microscopy, the coverslips were carefully removed and mounted on microscope slides with 5μL 4′,6-diamidino-2-phenylindole (DAPI) DNA stain.

Data Analysis

Statistical analysis was conducted using GraphPad Prism 6 statistical analysis software.

Results

Confocal Microscopy Produces High Variability

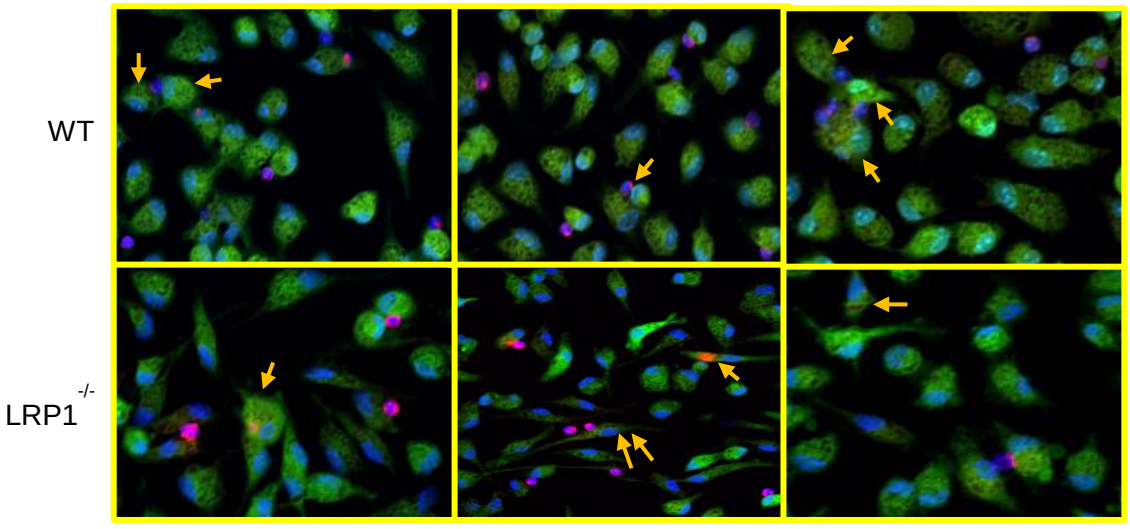

Figure 7. Confocal Microscopy was used to quantify phagocytic Index. Green labeled macrophages were co-incubated with red labeled apoptotic cells then imaged on a Nikon A1R Confocal Microscope. An efferocytosis event was counted when a macrophage contained or was in contact with an apoptotic cell, indicated by the yellow arrows. If a macrophage contained multiple apoptotic cells, or multiple macrophages were in contact with one apoptotic cell, each was counted as a separate event.

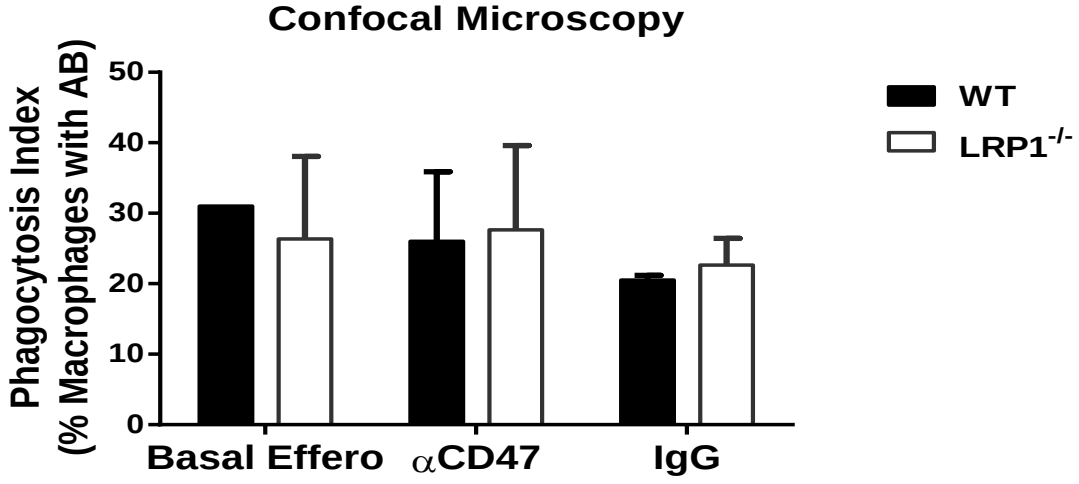

For confocal microscopy, primary macrophages (WT or LRP1$^{-/-}$) were seeded onto coverslips, labeled green, and co-incubated with violet labeled apoptotic Jurkat cells. Prior to co-incubation, and during apoptosis induction, the Jurkat cells received either the CD47 blocking antibody, IgG control or no treatment. The cells were imaged and counted as outlined in the methods section. The macrophages were extracted from three mice for each genotype and mixed. The cells were then seeded in triplicate into the wells. That is three slides per condition (n=3). When imaged, the slides showed a high degree of confluency. Therefore, a grid was overlaid on the image in ImageJ, and arbitrary grid sections were quantified. Five grid sections were selected, and the percent efferocytosis from each section were averaged. As will be discussed, there were imaging issues with the WT slides. This only allowed for quantification of n=1 for basal efferocytosis and n=2 for IgG and CD47 for the WT group. For the LRP1$^{-/-}$ slides n=3 for all groups.

Basal efferocytosis produced a high degree of variability in the LRP1$^{-/-}$ genotype. Two slides had values of 35% and 31% phagocytic index (PI) respectively, while one had 13% PI. Due to the issues with the WT slides only one was quantified for the basal condition yielding 31% PI. For the IgG group, the WT slides (n=2) had a PI of 33% and 19% respectively. The IgG LRP1$^{-/-}$ group (n=3) had 20%, 27%, and 21% PI. For the CD47 condition, WT (n=2) yielded 33% and 19% PI. The CD47 LRP1$^{-/-}$ group yielded 24%, 41%, and 18% PI. Due to the high variability of the results, no statistical tests were performed on these results.

Fluorescence Activated Cell Sorting (FACS)

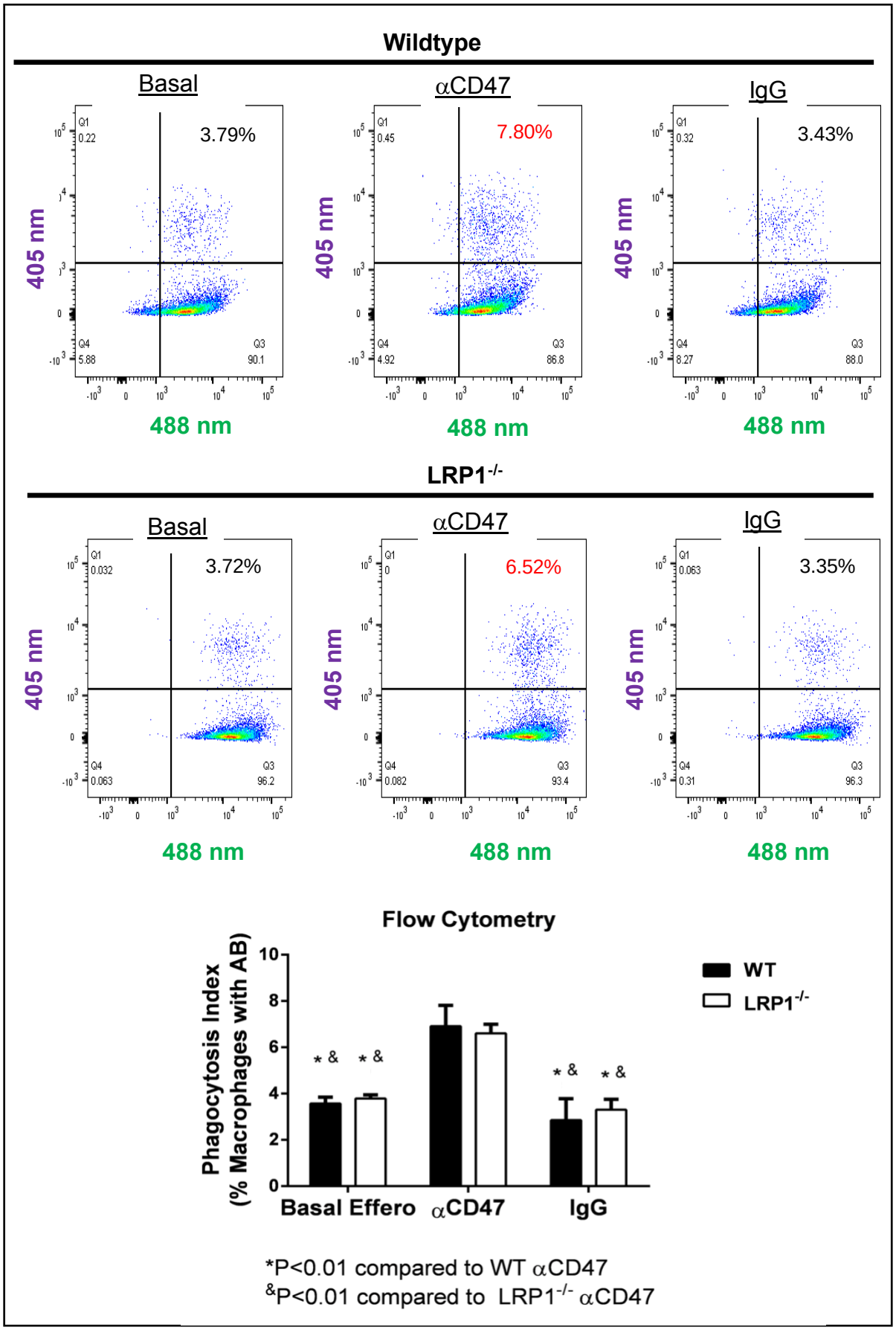
Wildtype
Basal
αCD47
IgG
3.79%
7.80%
3.43%
405 nm
488 nm
Q1 0.22
Q4 5.88
Q3 90.1
Q1 0.45
Q4 4.92
Q3 86.8
Q1 0.32
Q4 8.27
Q3 88.0
LRP1-/-
Basal
αCD47
IgG
3.72%
6.52%
3.35%
Q1 0.032
Q4 0.063
Q3 96.2
Q1 0
Q4 0.082
Q3 93.4
Q1 0.063
Q4 0.31
Q3 96.3
Flow Cytometry
Phagocytosis Index (% Macrophages with AB)
WT
LRP1-/-
Basal
Effero
αCD47
IgG
*P<0.01 compared to WT αCD47
&P<0.01 compared to LRP1-/- αCD47

FACS experiments were conducted concurrently with confocal microscopy experiments as outlined in the methods section. WT and LRP1$^{-/-}$ primary macrophages were seeded in triplicate (n=3) into wells and labeled green. Violet labeled Jurkat cells were exposed to IgG, αCD47, or no treatment, while exposed to UV light to induce apoptosis.

Statistical analysis was conducted on GraphPad Prism 6 using a two-way ANOVA with Sidak's multiple comparisons test. The results show that there is no difference in phagocytic index between WT and LRP1$^{-/-}$ genotypes for any of the treatment groups ($p < 0.01$). WT and LRP1$^{-/-}$ yielded 7.80% and 6.52% PI respectively. It is worth noting that the phagocytic index observed in these experiments is significantly lower than those observed in previous studies, discussed below.

Western Blot – MerTK

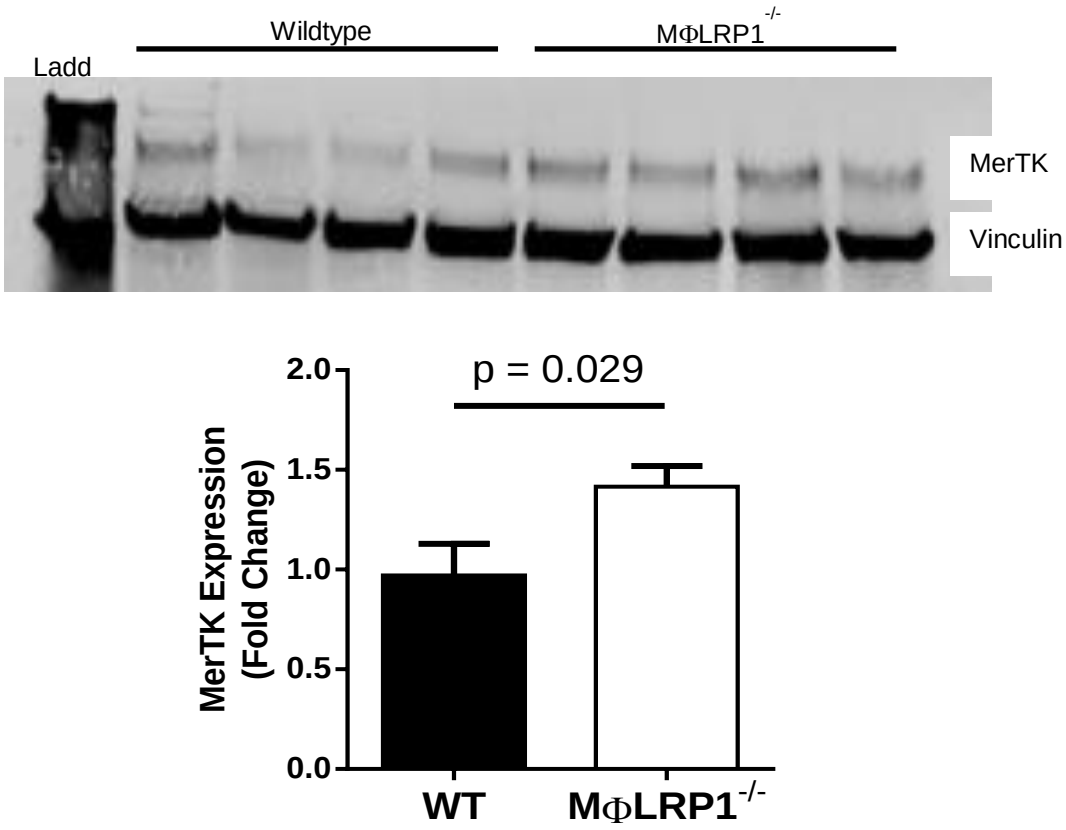

Protein expression of another pro-efferocytosis receptor, MerTK, was analyzed via Western blot to ascertain if other pro-efferocytosis receptors were upregulated and explain the results which were observed in the FACS results. This analysis was conducted on WT or LRP1$^{-/-}$ primary macrophages (MΦLRP$^{-/-}$) that were exposed to either a vehicle (Serum-Free DMEM) or IgG control.

Macrophages from three mice were collected for each genotype and divided into four replicates (n=4), and protein expression was quantified. A Mann-Whitney non-parametric test was conducted using GraphPad Prism 6. The results show a 1.46-fold increase in MerTK expression in the LRP1$^{-/-}$ group compared to the WT ($p = 0.029$).

Wild Type vs. LRP1 Substrate Experiments

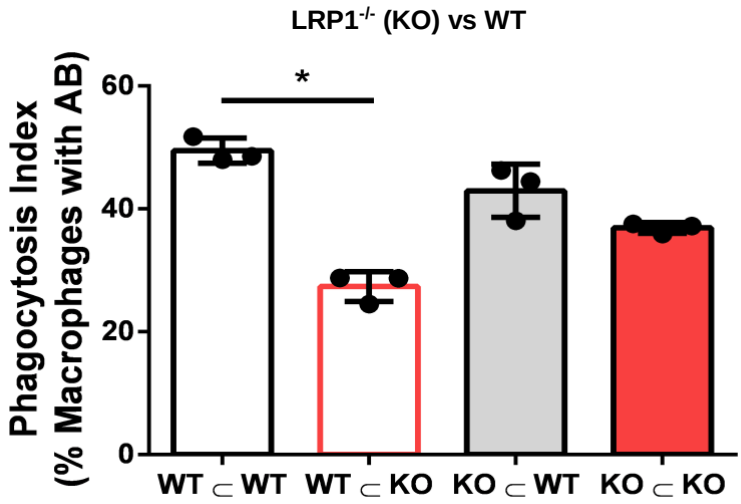

WT vs LRP1$^{-/-}$ efferocytosis experiments were conducted in order to gain insight into LRP1's effect on a cell's ability to be eaten. Primary macrophages from either WT or LRP1$^{-/-}$ (KO) macrophages were collected and seeded into well plates. Four experimental conditions were selected. WT phagocytosing WT or LRP1$^{-/-}$, and LRP1$^{-/-}$ phagocytosing WT or LRP1$^{-/-}$. Efferocyte were labeled with a green fluorescent probe and ACs were

labeled with a violet probe, as per previous experiments. For this experiment, the method of inducing apoptosis was changed to staurosporine, discussed below. To determine phagocytic index, FACS was performed.

A Kruskal-Wallis non-parametric one-way ANOVA, with Dunn's multiple comparison test, was conducted using GraphPad Prism 6. The results show a significant decrease (22%, $p < 0.0001$) in phagocytic index when a WT macrophage is phagocytosing an $LRP1^{-/-}$ knockout ACs when compared to a WT phagocytosing a WT ACs.

Discussion

First, it is important to discuss the results for confocal microscopy. As the data shows, there was a high degree of variability when we used this method. This variability was consistent throughout assay development and multiple experimental trials. Variability may be due to the small sample size. During the imaging process, some of the coverslips did not fluoresce and thus, could not be quantified. Despite this, the levels of variability have not been seen by other labs using a similar technique. However, due to our results, it was determined that confocal microscopy is not an effective assay to determine phagocytic index for efferocytosis in our model.

The results show that an LRP1 knockout does not affect efferocytosis given a CD47 blockade in our model. Therefore, we began to investigate factors which may explain our observations. First, we conducted Western blot analysis of another common pro-efferocytosis receptor, MerTK. Our results show that MerTK was upregulated approximately one and a half fold in the LRP1 knockout macrophages compared to the wild type and standardized to our loading control vinculin. Additionally, recent proteomics data generated in our lab shows that another pro-efferocytosis receptor,

CD36, is highly upregulated in LRP1 knockout macrophages compared to the wild type. Future studies will be conducted to determine the effect that these and other pro-efferocytosis factors have on efferocytosis.

The results from the FACS experiments also yielded a significantly lower phagocytic index than those established by other groups. This was thought to be due to the method of apoptosis induction, UV light. After these results, the method of apoptosis induction was changed to a chemical method, staurosporine. Changing the method of apoptosis induction brought the phagocytic index back in line with literature values as observed in the substrate experiment results.

We also conducted an experiment using WT or $LRP1^{-/-}$ macrophages as either apoptotic cell substrate (ACs) or efferocyte. This was done to determine the effect that LRP1 had on a cells ability to be eaten. As the results indicate, an apoptotic cell with LRP1 knocked out, results in a significantly lower phagocytic index when being phagocytosed by a macrophage which expresses LRP1. Because of these results, we plan to analyze a biological process known as autophagy.

As mentioned above, LRP1 is a multi-ligand receptor which plays a role in a wide range of biological processes. LRP1 has been implicated as a key receptor in autophagy (Grosso et al., 2019). Autophagy is the process by which a cell catabolizes and packages unnecessary cellular components (Glick, Barth, & Macleod, 2010). Links have been established between autophagy and apoptosis (Thorburn, 2008). Therefore, if LRP1 is not expressed on an apoptotic cell, this disrupts efficient packaging of the apoptotic cells' cellular components. The incoming efferocyte would have increased difficulty in phagocytosing the apoptotic cell.

Conclusion

The pro-efferocytosis receptor LRP1 is necessary for the athero-protective effect of an anti-CD47 antibody blockade *in vivo*. However, an LRP1 knockout with a CD47 blockade *in vitro* does not show impaired efferocytosis compared to the wild type in our model. Our subsequent protein expression analysis shows that this may be due to an increase in the expression of other pro-efferocytosis receptors. However, a decrease in efferocytosis is still seen *in vivo.* This decrease may be due to LRP1's role in autophagic flux, as discussed above. Therefore, we plan to conduct experiments that repeat the WT versus $LRP1^{-/-}$ substrate experiments in the presence of αCD47 and continue to measure the expression of other pro-efferocytosis receptors in an effort to better understand the mechanisms underlying the impaired efferocytosis seen in atherosclerosis.

References

Elliott, M. R., Koster, K. M., & Murphy, P. S. (2017). Efferocytosis Signaling in the Regulation of Macrophage Inflammatory Responses. *The Journal of Immunology, 198*(4), 1387-1394. Retrieved from https://dx.doi.org/10.4049/jimmunol.1601520. doi:10.4049/jimmunol.1601520

Fadok, V. A., Warner, M. L., Bratton, D. L., & Henson, P. M. (1998). CD36 Is Required for Phagocytosis of Apoptotic Cells by Human Macrophages That Use Either a Phosphatidylserine Receptor or the Vitronectin Receptor (αvβ3). *The Journal of Immunology*(161), 6250-6257.

Gardai, S. J., McPhillips, K. A., Frasch, S. C., Janssen, W. J., Starefeldt, A., Murphy-Ullrich, J. E., . . . Henson, P. M. (2005). Cell-surface calreticulin initiates clearance of viable or apoptotic cells through trans-activation of LRP on the phagocyte. *Cell, 123*(2), 321-334. Retrieved from https://www.ncbi.nlm.nih.gov/pubmed/16239148. doi:10.1016/j.cell.2005.08.032

Glick, D., Barth, S., & Macleod, K. F. (2010). Autophagy: cellular and molecular mechanisms. *J Pathol, 221*(1), 3-12. Retrieved from https://www.ncbi.nlm.nih.gov/pubmed/20225336. doi:10.1002/path.2697

Grosso, R. A., Caldarone, P. V. S., Sanchez, M. C., Chiabrando, G. A., Colombo, M. I., & Fader, C. M. (2019). Hemin induces autophagy in a leukemic erythroblast cell line through the LRP1 receptor. *Biosci Rep, 39*(1). Retrieved from https://www.ncbi.nlm.nih.gov/pubmed/30523204. doi:10.1042/BSR20181156

Kasikara, C., Doran, A. C., Cai, B., & Tabas, I. (2018). The role of non-resolving inflammation in atherosclerosis. *Journal of Clinical Investigation, 128*(7), 2713-2723. Retrieved from https://dx.doi.org/10.1172/JCI97950. doi:10.1172/jci97950

Kojima, Y., Volkmer, J.-P., McKenna, K., Civelek, M., Lusis, A. J., Miller, C. L., . . . Leeper, N. J. (2016). CD47-blocking antibodies restore phagocytosis and prevent atherosclerosis. *Nature, 536*(7614), 86-90. Retrieved from https://dx.doi.org/10.1038/nature18935. doi:10.1038/nature18935

Kojima, Y., Weissman, I. L., & Leeper, N. J. (2017). The Role of Efferocytosis in Atherosclerosis. *Circulation, 135*(5), 476-489. Retrieved from https://www.ncbi.nlm.nih.gov/pubmed/28137963. doi:10.1161/CIRCULATIONAHA.116.025684

Linton, M. F., Yancey, P. G., Davies, S. S., Jerome, W. G. J., Linton, E. F., & Vickers, K. C. (2015). The Role of Lipids and Lipoproteins in Atherosclerosis. In K. Feingold & D. P. Wilson (Eds.), *Endotext.org*. South Dartmouth, MA: MDText.com, Inc.

Majeti, R., Chao, M. P., Alizadeh, A. A., Pang, W. W., Jaiswal, S., Kenneth D. Gibbs, J., . . . Weissman, I. L. (2009). CD47 is an adverse prognostic factor and therapeutic antibody target on human acute myeloid leukemia stem cells. *Cell, 138*(2), 286-299. Retrieved from https://www.ncbi.nlm.nih.gov/pubmed/19632179. doi:10.1016/j.cell.2009.05.045

Moore, K. J., Sheedy, F. J., & Fisher, E. A. (2013). Macrophages in atherosclerosis: a dynamic balance. *Nature Reviews Immunology, 13*(10), 709-721. Retrieved from https://dx.doi.org/10.1038/nri3520. doi:10.1038/nri3520

Moore, K. J., & Tabas, I. (2011). Macrophages in the pathogenesis of atherosclerosis. *Cell, 145*(3), 341-355. Retrieved from https://www.ncbi.nlm.nih.gov/pubmed/21529710. doi:10.1016/j.cell.2011.04.005

Overton, C. D., Yancey, P. G., Major, A. S., Linton, M. F., & Fazio, S. (2007). Deletion of macrophage LDL receptor-related protein increases atherogenesis in the mouse. *Circulation Research, 100*(5), 670-677. Retrieved from https://www.ncbi.nlm.nih.gov/pubmed/17303763. doi:10.1161/01.RES.0000260204.40510.aa

Saladin, K. (2012). *Anatomy & Physiology: The Unity of form and function* (6 ed.). New York, NY: McGraw Hill.

Seimon, T., & Tabas, I. (2009). Mechanisms and consequences of macrophage apoptosis in atherosclerosis. *Journal of Lipid Research, 50 Suppl*, S382-387. Retrieved from https://www.ncbi.nlm.nih.gov/pubmed/18953058. doi:10.1194/jlr.R800032-JLR200

Tabas, I. (2010). Macrophage death and defective inflammation resolution in atherosclerosis. *Nature Reviews Immunology, 10*(1), 36-46. Retrieved from https://www.ncbi.nlm.nih.gov/pubmed/19960040. doi:10.1038/nri2675

Tabas, I. (2016). Death-defying plaque cells. *Nature, 536*(7614), 32-33. Retrieved from https://dx.doi.org/10.1038/nature18916. doi:10.1038/nature18916

Thorburn, A. (2008). Apoptosis and autophagy: regulatory connections between two supposedly different processes. *Apoptosis, 13*(1), 1-9. Retrieved from https://www.ncbi.nlm.nih.gov/pubmed/17990121. doi:10.1007/s10495-007-0154-9

Thorp, E., Cui, D., Schrijvers, D. M., Kuriakose, G., & Tabas, I. (2008). Mertk receptor mutation reduces efferocytosis efficiency and promotes apoptotic cell accumulation and plaque necrosis in atherosclerotic lesions of apoe-/- mice. *Arterioscler Thromb Vasc Biol, 28*(8), 1421-1428. Retrieved from https://www.ncbi.nlm.nih.gov/pubmed/18451332. doi:10.1161/ATVBAHA.108.167197

WHO. (2018). The top 10 causes of death. Retrieved from https://www.who.int/news-room/fact-sheets/detail/the-top-10-causes-of-death

Yancey, P. G., Blakemore, J., Ding, L., Fan, D., Overton, C. D., Zhang, Y., . . . Fazio, S. (2010). Macrophage LRP-1 Controls Plaque Cellularity by Regulating Efferocytosis and Akt Activation. *Arteriosclerosis, Thrombosis, and Vascular Biology, 30*(4), 787-795. Retrieved from https://dx.doi.org/10.1161/ATVBAHA.109.202051. doi:10.1161/atvbaha.109.202051

Yancey, P. G., Ding, Y., Fan, D., Blakemore, J. L., Zhang, Y., Ding, L., . . . Fazio, S. (2011). Low-Density Lipoprotein Receptor-Related Protein 1 Prevents Early Atherosclerosis by Limiting Lesional Apoptosis and Inflammatory Ly-6Chigh Monocytosis: Evidence That the Effects Are Not Apolipoprotein E Dependent. *Circulation, 124*(4), 454-464. Retrieved from https://dx.doi.org/10.1161/CIRCULATIONAHA.111.032268. doi:10.1161/circulationaha.111.032268